Available online at www.sciencedirect.com
SCIENCE DIRECT
Journal of Power Sources 158 (2006) 735–739
JOURNAL OF POWER SOURCES
www.elsevier.com/locate/jpowsour

Short communication

Oxygen reduction reaction on nanosized manganese oxide particles dispersed on carbon in alkaline solutions

M.L. Calegaro *, F.H.B. Lima, E.A. Ticianelli

Instituto de Química de São Carlos, Universidade de São Paulo, Avenida Trabalhador Sancarlense, 400 Parque Arnold Schmidt, CP 780 13560-970 São Carlos, SP, Brazil

Received 23 June 2005; received in revised form 18 August 2005; accepted 31 August 2005
Available online 16 November 2005

Abstract

In this work a manganese oxide dispersed on a high surface area carbon powder at two ratios (Mn_yO_x/C) was evaluated as catalyst for the oxygen reduction reaction (ORR) in alkaline solutions. An impregnation method was used to prepare the catalysts, starting from a manganese nitrate precursor solution containing the carbon powder (Vulcan XC-72). A thin porous coating rotating disk electrode was employed to collect the experimental ORR polarization data and the results obtained were analyzed with the application of the flooded-agglomerate/thin film model for the catalyst layer. Results indicated that the reaction is sensitive to the manganese oxide to carbon ratio on the catalyst. The catalyst containing lower Mn_yO_x/C ratio tended to follow the peroxide pathway ($2e^-$ mechanism) forming peroxide ions. When the Mn_yO_x content is increased the complete reduction of oxygen to hydroxide ions pathway (the $4e^-$ mechanism) takes place into some extent at low potentials due to the occurrence of a catalytic disproportionation of HO_2^-.

Keywords: ORR; Alkaline solutions; Flooded-agglomerate/thin film model; Manganese oxide catalysts

1. Introduction

One of the most studied processes in electrochemistry is the cathodic reduction of molecular oxygen, either in alkaline or in acid solutions, due to the importance of this reaction for fuel cells [1] and metal-air batteries [2]. The most effective catalyst used to promote the oxygen reduction reaction (ORR) kinetics is a material formed by platinum-based particles highly dispersed on a high surface area substrate (normally a carbon powder). However, Pt-based catalysts are very expensive, and additionally suffer gradual decrease in activity. These aspects have motivated the development of alternative materials that have been successfully employed on the ORR, particularly in the construction of cathodes for alkaline fuel cells and metal-air batteries [3,4].

The main challenge related to the development of high active catalysts for the ORR is to obtain a material capable of achieving the complete reduction process, where a four-electron transfer per O_2 is involved. However, some of the catalysts reported in the literature accelerate a two-electron reduction of O_2 to produce H_2O_2. Manganese oxide is among the most widely used catalyst for the ORR in alkaline metal-air batteries [5–8]. One of the functions of this oxide is to perform the decomposition of hydrogen peroxide, which is formed during the electrochemical reduction of oxygen [8], by a disproportionation mechanism conducting the ORR to follow the complete reduction pathway, where a $4e^-$ transfer per oxygen molecule is obtained.

The objective of the present work is to further demonstrate the efficiency of a manganese oxide as catalyst for the ORR in alkaline solutions (1.0 mol L^{-1} NaOH). In order to obtain high specific area, the catalyst was obtained in the form of a highly dispersed powder supported on carbon following an impregnation method as suggested by Lamminen et al. [9]. The method involves the use of a nitrate precursor ($Mn(NO_3)_2{\cdot}4H_2O$), which is thermally decomposed to produce very small metal oxide particles. Since the resulting material is a non-stoichiometric metal oxide (see details in Section 2) it will be represented as Mn_yO_x/C. This catalyst was characterized by XRD (X-ray diffraction) measurements, while cyclic voltammetry and steady-state polarization techniques were employed

* Corresponding author. Fax: +55 16 3373 9952.
E-mail address: calegaro@iqsc.usp.br (M.L. Calegaro).

0378-7753/$ – see front matter © 2005 Elsevier B.V. All rights reserved.
doi:10.1016/j.jpowsour.2005.08.048

for the ORR investigations. The electrodes were constructed using the thin porous coating rotating disk (TPC) technique [10]. The steady-state oxygen reduction polarization data collected by this technique were analyzed using the thin film/flooded-agglomerate model of gas diffusion electrode, as mathematically treated in the Cartesian system by Springer and Raistrick [11,12].

2. Experimental

The Mn_yO_x/C catalyst was obtained by thermal decomposition of manganese nitrate, following a procedure described by Lamminen et al. [9]. Two different compositions were prepared, one with low manganese oxide load (Mn_xO_y/C_{LL}) and the other with high oxide content (Mn_xO_y/C_{HL}). The mass of manganese in the Mn_xO_y/C_{HL} catalyst was calculated in order to be twice that in the Mn_xO_y/C_{LL}. The physical characterization of the catalysts was carried out by XRD analysis using a Philips diffractometer with the Cu Kα characteristic radiation, in the 2θ range from 20° to 80° at 2° min^{-1}. In order to estimate the mean particle size of the catalysts the XRD results were analyzed by the *WinFit* software [13]. This is a program for profile analysis of X-ray reflections and peak fittings, which can be used to obtain the particle size and strain information of the investigated sample.

Thin porous coating rotating disk electrodes were used for cyclic voltammetry and polarization measurements. The electrodes were prepared by mixing the catalyst powders with a dilute suspension (≈2%, w/w) of a Teflon emulsion (Du Pont TM 30) and following the procedure described elsewhere [10]. A conventional one-compartment cell was used for the electrochemical experiments. A platinum foil and a saturated calomel electrode (SCE) were used as counter and reference electrodes, respectively. All the experiments were carried out in 1.0 mol L^{-1} NaOH solutions prepared from high purity sodium hydroxide pellets (Mallinckrodt) and distilled water further purified in a Milli-Q (Millipore) system. The electrolyte was saturated with purified N_2 (White & Martins) 99.96% for the cyclic voltammetric experiments or O_2 (White & Martins) 99.995% for the experiments involving the ORR.

The cyclic voltammetry and rotating disk polarization measurements were performed in a Princeton Applied Research (PAR) 273-A potentiostat coupled with an IBM-PC compatible microcomputer. The electrode rotation speeds were controlled by an AFMSRE/ASR system from the Pine Instrument Company. The oxygen reduction polarization curves involving the TPC electrodes were recorded point-by-point in the potentiostatic mode. This procedure helps to minimize the high capacitive currents associated to this type of electrode. All the experiments were conducted at room temperature (25 ± 1 °C).

3. Results and discussion

3.1. Physical characterization

Fig. 1b shows XRD patterns obtained for the Mn_yO_x/C catalysts. The result obtained for a 10 wt.% Pt/C catalyst (E-Tek) is included for comparisons. These results indicate that the catalyst is crystalline and composed by a mixture of manganese oxides, β-MnO_2 and Mn_2O_3. One of the most used methods to prepare manganese oxides is the thermal decomposition of suitable chemical precursors, including nitrate [9], acetate [14], carbonate [15], sulfate [15], etc. The resulting product depends on the precursor used and of the experimental conditions (decomposition temperature [16], moisture content of the atmosphere [17], hydration degree of the nitrates [18], crystal size and support [19]). The mechanism of thermal decomposition of manganese nitrate in air atmosphere (as in this work) was comprehensively studied by Hussein and co-workers [16]. According to this work, until 220 °C the precursor is converted to MnO_2 which is quantitatively converted to Mn_2O_3 at 560 °C. A mixture of MnO_2 and Mn_2O_3 is expected when the thermal decomposition of $Mn(NO_3)_2$ is conducted at temperatures below 560 °C, as demonstrated by the XRD patterns in Fig. 1b. The presence of β-MnO_2 in the catalyst is also in agreement with other results available in the literatures [9,16].

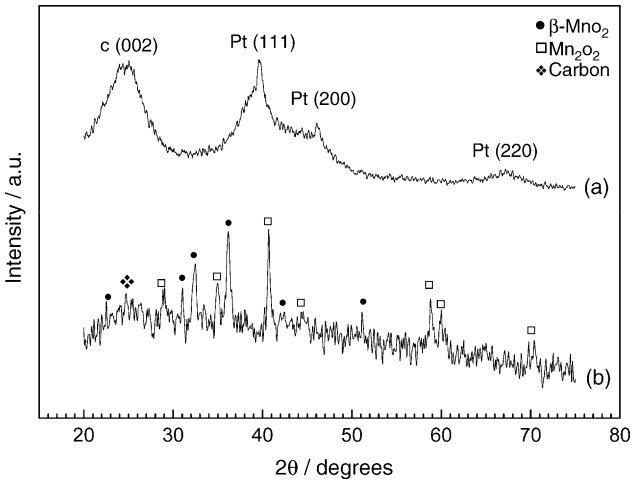

Fig. 1. X-ray diffraction patterns for: (a) 10% Pt/C (E-TEK Inc., USA) and (b) Mn_xO_y/C_{LL} electrodes.

There in no previous report about the particle size of manganese oxides obtained by impregnation, so the XRD results were also analyzed using the WinFit [13] software in order to estimate the mean crystallite size of the catalyst particles. The software allows modeling a peak by one or more profile shape functions and the size-distribution is determined from the second derivative of the Fourier-coefficient plots. To evaluate the derivative, a Savitzky–Golay polynomial was used. In order to validate the method, the same procedure was used for the XRD obtained for a 10 wt.% Pt/C (E-Tek USA) as depicted in Fig. 1. The result obtained from this calculation indicated a mean crystallite size of Pt equals to 2.4 nm, in quite good agreement with that presented previously [20] (2.3 nm). The mean crystallite size was estimated by WinFit for Mn_xO_y/C as being around 15 nm. Such result clearly demonstrates the large surface area of the Mn_xO_y/C catalyst, fulfilling a basic requirement for application on gas diffusion electrodes.

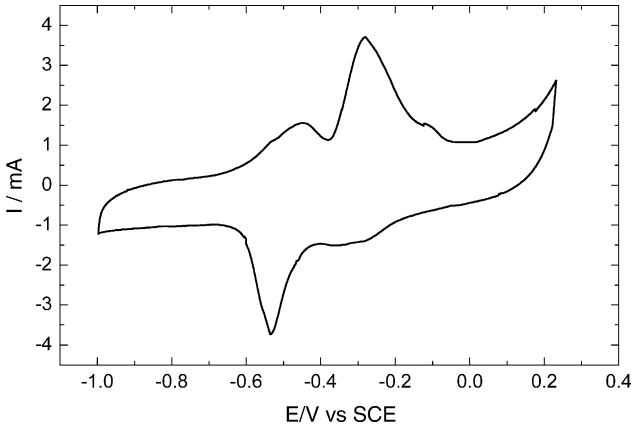

Fig. 2. Cyclic voltammograms obtained in 1.0 mol L^{-1} NaOH solution for the Mn_xO_y/C_{LL} electrode obtained experimentally by thermal decomposition of manganese nitrate ($v = 10$ mV s^{-1}).

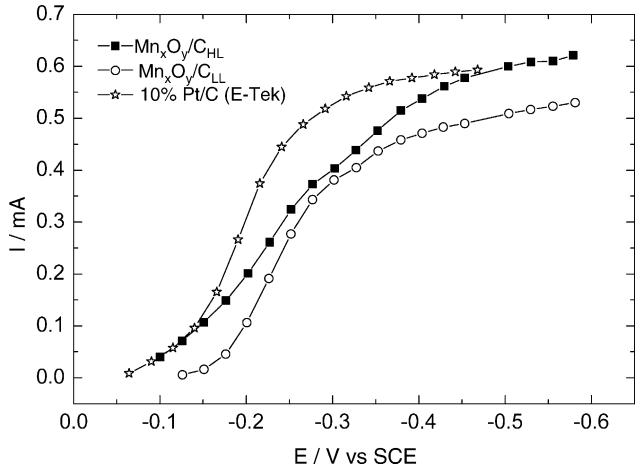

Fig. 3. Steady-state polarization curves for oxygen reduction in 1.0 mol L^{-1} NaOH solution on TPC-RDE prepared with different catalysts.

3.2. Cyclic voltammetry

Fig. 2 shows the cyclic voltammogram (cv) profile for the Mn_yO_x/C_{LL} TPC electrode recorded at a scan rate of 10 mV s^{-1}. The voltammetric profile is very similar to those found in the literatures [21–23] and the voltammetric peaks are associated to a series of redox processes [22,23]. These processes are composed of several steps and the corresponding voltammetric peaks are overlapped and difficult to identify or to associate with a specific process. Meanwhile the main reactions are those associated to the reduction and reoxidation of MnO_2 and Mn_2O_3. The reduction reaction of MnO_2 is composed by two consecutive steps, Mn^{IV}/Mn^{III} and Mn^{III}/Mn^{II}:

$$MnO_2 + H_2O + e^- \rightarrow MnOOH + OH^- \quad (1)$$

$$MnOOH + H_2O + e^- \rightarrow Mn^{2+} + 3OH^- \quad (2)$$

Reaction (2) indicated above might be considerably suppressed, or completely inhibited, by resistive effects, due to the poor conductivity of MnOOH. It may involve partial dissolution of MnOOH and disproportionation into MnO_2 and Mn^{2+}. The reduction reaction of Mn_2O_3 occurs into a unique step according to

$$Mn_2O_3 + 3H_2O + 2e^- \rightarrow 2Mn(OH)_2 + 2OH^- \quad (3)$$

and its oxidation leads to the production of MnO_2 according to [24]:

$$Mn_2O_3 + 2OH^- \rightarrow 2MnO_2 + H_2O + 2e^- \quad (4)$$

The experimental procedure used to produce the catalyst in this work is very adequate to prepare nanosized oxide particles, providing an efficient contact between the catalyst particles and the carbon powder substrate. The experimental method is also very suitable in the sense that very stable and reproducible voltammetric response is obtained, even after more than 20 consecutive cycles.

3.3. Electrochemical reduction of oxygen

The use of manganese oxides as catalysts for the electrochemical reduction of oxygen had been the subject of several previous works [8,25–27], exploring the effects of different aspects of the oxide properties, such as crystallographic phase [26] and the manganese oxidation state [8]. Fig. 3 presents the steady-state polarization curves obtained at 1600 rpm for the ORR on Mn_yO_x/C catalysts with different manganese oxide loads. The results clearly indicate an enhancement of the catalytic activity as the amount of manganese oxide is increased. At low current densities the performance of the catalysts with higher content of manganese oxides is almost the same as for 10% Pt/C.

The mass transport corrected Tafel curves (E versus $\log[(I \times I_d)/(I_d - I)]$, where I_d is the diffusion limiting current) for both manganese oxide electrodes are presented in Fig. 4. Two linear regions at low and high overpotentials are observed for both electrodes, with the slopes at high overpotential ($b_{LL} = 114$ mV decade^{-1}; $b_{HL} = 240$ mV decade^{-1}) being twice that at low overpotentials ($b_{LL} = 57$ mV decade^{-1};

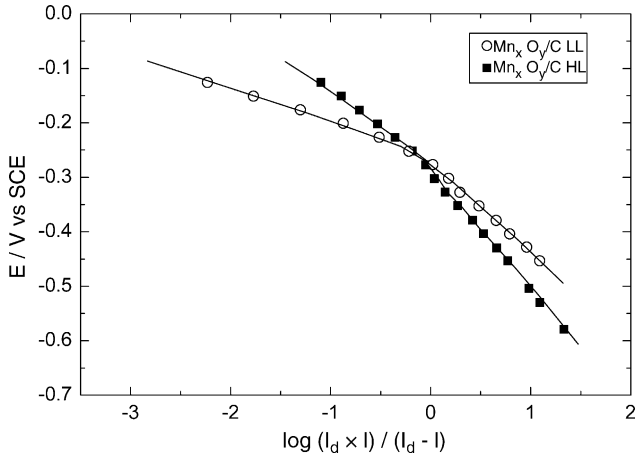

Fig. 4. Experimental (symbols) and simulated (solid lines) Tafel plots for the oxygen reduction on different catalysts in 1.0 mol L^{-1} NaOH solution ($\omega = 1600$ rpm).

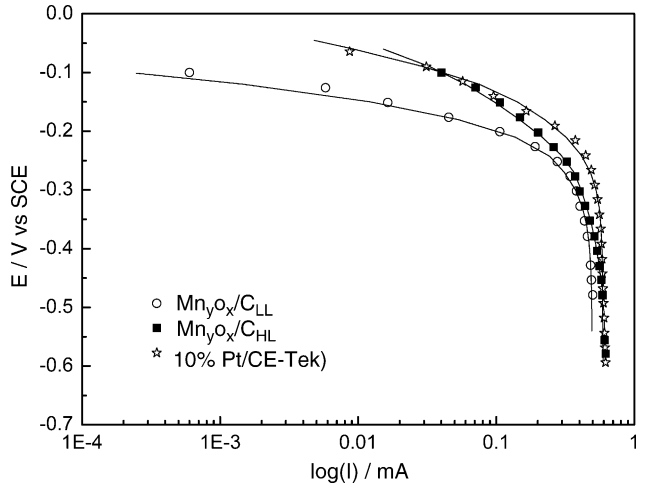

Fig. 5. Mass-transport corrected Tafel plots for oxygen reduction on the Mn_xO_y/C catalysts in 1.0 mol L^{-1} NaOH solution ($\omega = 1600$ rpm). Solid line: simulated Tafel plot; symbols: experimental data.

$b_{HL} = 120$ mV $decade^{-1}$). It was already demonstrated [28] that the existence of two linear regions in the polarization curves of TPC electrodes is exclusively related to structural effects of the catalyst layer and not to changes on the reaction pathway. Following this suggestion the increase of b resulting when the amount of manganese oxide is increased may be assigned to difficulties of oxygen diffusion and/or to ohmic effects.

In order to analyze quantitatively this point, the steady-state oxygen reduction polarization data were analyzed using the flooded-agglomerate/thin film model of gas diffusion electrode, as mathematically treated in the Cartesian system by Springer and Raistrick [11,12,28]. The experimental and simulated curves are presented in Fig. 5 and the corresponding kinetic parameters for the oxygen reduction reaction (free from oxygen diffusion effects) obtained from the simulated curves are presented in Table 1. Results for 10 wt.% Pt/C are included for comparison.

Results presented in Table 1 clearly indicate that the Tafel slope for the ORR in the high oxide load electrode is twice that seen for the low loading electrode. Also in each case, only one value of slope is necessary to simulate the experimental response for the entire range of potentials or current densities, indicating that the changes of b as function of the current density observed in Fig. 4 are caused by oxygen diffusion limitations in the flooded agglomerate [11,12,28].

Since for both Mn_xO_y/C electrodes the active material is the same, the difference in the Tafel slope between the low and high oxide load electrodes cannot be associated to a change on the reaction pathway. Also, the change cannot be related to diffusion problems in the flooded agglomerate, because this phenomenon is compensated by the modeling procedure so that the resulting value of b (Table 1) is that free from this effect. Thus, it is proposed that the larger slopes obtained for Mn_xO_y/C_{HL} can only be due to an increased ohmic effect arising from the large Mn_xO_y/C content, which decreases the conductivity of the electrodic composite [11,12,28].

Table 1
Fitting parameters obtained for oxygen reduction on Mn_xO_y/C in 1.0 mol L^{-1} NaOH at 25 °C

Composition	n	b (mV $decade^{-1}$)	i_0 (A cm^{-2})
Mn_xO_y/C_{LL}	2.1	57	2.6×10^{-11}
Mn_xO_y/C_{HL}	2.8	120	7×10^{-10}
10 wt.% Pt/C (E-Tek)	2.8	47	2×10^{-10}

It is also seen from Table 1 that n increases as the manganese oxide content in the catalyst layer increases. As demonstrated before for the case of Pt/C catalysts with several platinum-to-carbon ratios [28,29], this is an indication that the carbon substrate may also participate in the oxygen reduction, where the reaction proceeds through the peroxide pathway [30] according to

$$O_2 + H_2O + 2e^- \rightarrow HO_2^- + OH^- \quad (5)$$

which in the presence of manganese oxide may be followed by heterogeneous catalytic decomposition of hydrogen peroxide [8,27]:

$$2HO_2^- \xrightarrow{Mn_xO_y/C} O_2 + 2OH^- \quad (6)$$

When the load of manganese oxide is low the reaction proceeds mainly on the carbon surface and only a negligible portion of the hydrogen peroxide is decomposed on the manganese oxide surface resulting in $n = 2.1$. An increase of the Mn_xO_y/C load leads to an increase of the number of electrons for the ORR indicating that the catalytic decomposition of hydrogen peroxide is more effective [8]. This effect can be also conveniently evaluated by Koutecký–Levich (K–L) plots constructed from the data in kinetic region (low overpotentials) of the polarization curves obtained at different rotation speeds. These plots are shown in Fig. 6. The slope of the K–L plots is directly related to the number of electrons involved in the reaction, the higher is the slope the lower is the number of electrons [31].

Fig. 6 shows that the behavior of the composites is very distinct from each other. The plots corresponding to the catalyst containing lower oxide load (Fig. 6a) show straight and parallel lines for different electrode potentials, indicating that the oxygen reduction reaction is first-order with respect to the reactant species and that the number of electrons involved in the reaction is the same, independent of the electrode potential. The situation is different for the Mn_xO_y/C_{HL} catalyst (Fig. 6b). The K–L plots for this catalyst are composed of straight lines whose slope increases with the increase of electrode potential, indicating that the number of electrons decrease as the overpotential increases. In Fig. 6c it is seen that the slope of the curve obtained at low potentials for the catalyst containing lower oxide load is higher than the slope for the higher load. In this sense these results are in complete agreement with the kinetics parameters presented in Table 1 and gives further support for the occurrence of the $2e^-$ mechanism followed by the disproportionation of OH_2^-.

The hydrogen peroxide disproportionation process may be composed by the following oxi-reduction steps, taking place by collision of two OH_2^- species at neighbor catalyst active sites:

$$HO_2^- + 2OH^- \rightarrow O_2 + H_2O + 2e \quad (7)$$

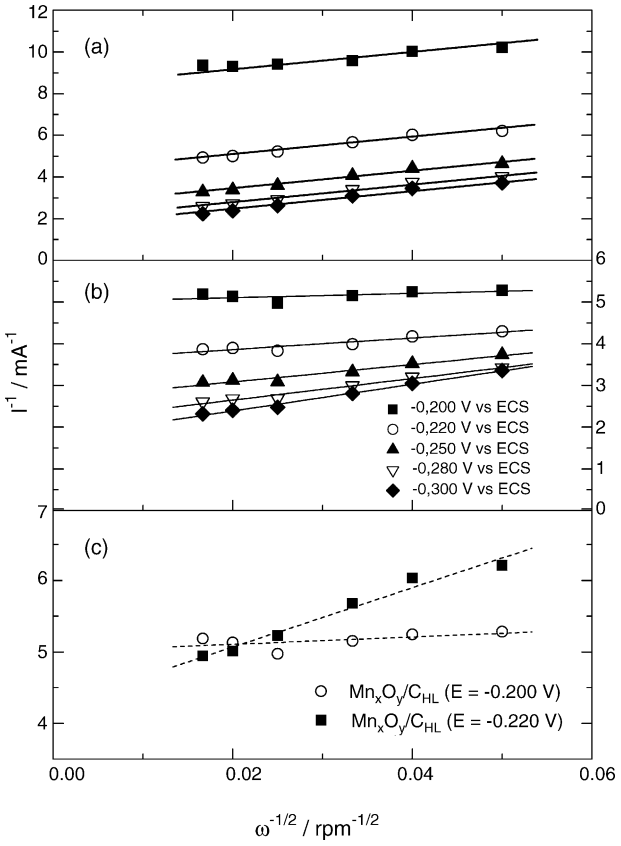

Fig. 6. Koutecký–Levich plots for oxygen reduction reaction in 1.0 mol L^{-1} NaOH solution at different potentials on: (a) Mn$_x$O$_y$/C$_{LL}$; (b) Mn$_x$O$_y$/C$_{HL}$ catalysts; (c) comparison of the results for both oxides.

$$HO_2^- + H_2O + 2e^- \rightarrow 3OH^- \quad (8)$$

where reaction (7) is just the reverse of reaction (5). Thus, the suppression of the OH_2^- disproportionation at high overpotentials for Mn$_x$O$_y$/C$_{HL}$ can be attributed to the fact that under this condition the oxidation of the peroxide ion (reaction (7)) back to O_2 is thermodynamically or kinetically retarded. Therefore, the overall process involving more than two electrons may only occur near the equilibrium potential for the peroxide reduction step ($E = -0.063$ V versus Hg/HgO) as confirmed by the results in Fig. 6b.

4. Conclusions

The activity of manganese oxide dispersed on carbon powder was investigated for the oxygen reduction reaction in alkaline solution using conventional electrochemical techniques and also by the application of the flooded-agglomerate model to the experimental ORR steady-state polarization data. Results indicate that the reaction proceeds through the peroxide route when the Mn$_x$O$_y$ load is small and that the carbon substrate may also contribute to the catalysis of the ORR. However, it was seen that when the load of manganese oxides is high heterogeneous catalytic hydrogen peroxide decomposition takes place, raising the number of electrons involved in the reaction, particularly near the equilibrium potential for the peroxide reduction step.

Acknowledgments

The authors wish to thank Fundação de Amparo à Pesquisa do Estado de São Paulo (FAPESP), Conselho Nacional de Desenvolvimento Científico e Tecnológico (CNPq) and Coordenação de Aperfeiçoamento de Pessoal de Nível Superior (CAPES) for financial supports.

References

[1] S. Srinivasan, J. Electrochem. Soc. 136 (1989) 41C.
[2] C. Chakkaravarth, A.K. Abdul Waheed, H.V.K. Udupa, J. Power Sources 6 (1981) 203–228.
[3] L. Swette, N. Kackley, J. Power Sources 29 (1990) 423–436.
[4] J. Kivisaari, J. Lamminen, J. Lampinen, M. Viitanen, J. Power Sources 32 (1990) 223–241.
[5] J.P. Hoare, The Electrochemistry of Oxygen, Wiley, 1968.
[6] T. Yano, D.A. Tryk, K. Hashimoto, A. Fujishima, J. Electrochem. Soc. 145 (1998) 1870.
[7] T. Yano, E. Popa, D.A. Tryk, K. Hashimoto, A. Fujishima, J. Electrochem. Soc. 146 (1999) 1081.
[8] L. Mao, D. Zhang, T. Sotomura, K. Nakatsu, N. Koshiba, T. Ohsaka, Electrochim. Acta 48 (2003) 1015–1021.
[9] J. Lamminen, J. Kivisaari, J. Lampinen, M. Viitanen, J. Vuorisalo, J. Electrochem. Soc. 138 (1991) 905–908.
[10] A.A. Tanaka, C. Fierro, D. Scherson, E.B. Yeager, J. Phys. Chem. 91 (1987) 3799.
[11] T.E. Springer, I.D. Raistrick, J. Electrochem. Soc. 134 (1989) 1594.
[12] I.D. Raistrick, Electrochim. Acta 35 (1990) 1579.
[13] S. Krumm, Comput. Geosci. 25 (1999) 489–499.
[14] A.E. Newkirk, Thermochim. Acta 2 (1971) 1.
[15] D. Dollimore, K.H. Tonge, in: G.-M. Schwab (Ed.), Proceedings of the Fifth International Symposium on the Reactivity of Solids, Elsevier, Amsterdam, 1965, pp. 497–508.
[16] A.K.H. Nohman, H.M. Ismail, G.A.M. Hussein, J. Anal. Appl. Pyrol. 34 (1995) 265–278.
[17] P.K. Gallagher, F. Schrey, B. Prescott, Thermochim. Acta 2 (1971) 405.
[18] M. Maneva, N. Petroff, J. Therm. Anal. 36 (1990) 2511.
[19] T. Cseri, S. Bekassy, G. Kenessey, G. Liptay, F. Figueras, Thermochim. Acta 288 (1996) 137.
[20] F. Maillard, M. Martin, F. Gloaguen, J.-M. Léger, Electrochim. Acta 47 (2002) 3431.
[21] J. McBreen, Electrochim. Acta 20 (1975) 221.
[22] P. Bezdicka, T. Grygar, B. Klapste, J. Vondrák, Electrochim. Acta 45 (1999) 913.
[23] P. Ruetschi, J. Electrochem. Soc. 123 (1976) 495.
[24] B. Klapste, J. Vondrák, J. Velická, Electrochim. Acta 47 (2002) 2365.
[25] Z. Wei, W. Huang, S. Zhang, J. Tan, J. Power Sources 91 (2000) 83–85.
[26] Y.L. Cao, H.X. Yang, X.P. Ai, L.F. Xiao, J. Electroanal. Chem. 557 (2003) 127.
[27] L. Mao, T. Sotomura, K. Nakatsu, N. Koshiba, D. Zhang, T. Ohsaka, J. Electrochem. Soc. 149 (4) (2002) A504–A507.
[28] J. Perez, E.R. Gonzalez, E.A. Ticianelli, Electrochim. Acta 44 (1998) 1329.
[29] J. Perez, A.A. Tanaka, E.R. Gonzalez, E.A. Ticianelli, J. Electrochem. Soc. 141 (1994) 431.
[30] E. Yeager, Electrochim. Acta 29 (1984) 1527.
[31] T. Ohsaka, L. Mao, K. Arihara, T. Sotomura, Electrochem. Commun. 6 (2004) 273.